POSTPRINT VERSION. The final version is published here :
Caza-Szoka, M., Massicotte, D. et Nougarou, F. (2018, 24-27 June 2018). Beamforming for Powerline Interference in Large Sensor Arrays. Communication présentée 2018 16th IEEE International New Circuits and Systems Conference (NEWCAS), Montreal, Canada. doi: 10.1109/NEWCAS.2018.8585510

BEAMFORMING FOR POWERLINE INTERFERENCE IN LARGE SENSOR ARRAYS

Manouane Caza-Szoka, Daniel Massicotte, François Nougarou

Université du Québec à Trois-Rivières, Electrical and Computer Engineering Department
C.P. 500, Trois-Rivières, Québec, Canada, G9A 5H7, www.uqtr.ca/lssi
{manouane.caza-szoka, daniel.massicotte, nougarou}@uqtr.ca

Abstract – This paper shows how to use beamforming to remove the power-line interference (PLI) in large surface electromyography (sEMG) sensor array or high-density sEMG. The method exploits the highly correlated nature of the different sources of interference, being part of the same electrical grid, and their narrow frequency bands. The idea is to use a very narrow pass-band filter around 50 or 60 Hz to get signals with high PLI content before applying a spatial filtering by principal component analysis (PCA). This way, beamforming are done on the frequency bands where PLI are presents. Also, it ensures that even if the PLI has a smaller overall power than the desired signal, it will be easily found as the most powerful component of the decomposition. The PLI can then be removed from the signal. With trivial modification, harmonics of the PLI can also be removed. The approach was used in the context of muscle behavior analyses of low back pain patients using a sEMG array of 64 sensors. The performances of the filter are studied by experimental and semi-empirical methods. Compared to the usual notch filter, an improvement of up 10 dB is found.

Index Terms— *sEMG, PLI, PCA, Spatio-Frequency Filtering, Large Sensor Arrays, EMG, EEG, ECG.*

1. INTRODUCTION

Surface electromyography (sEMG), by detecting electrical potential generated by activated muscle cells, is an effective non-invasive method widely used in biomedical research. Time- and frequency-domain methods have been developed to analyze the sEMG response in order to give information about muscle contraction and muscle fatigue necessary to study neuromuscular human diseases and behaviors. However, sEMG signals and its extracted information are strongly contained by different kinds of noises and artifacts like power-line interferences (PLI), sEMG sensor movements or electrocardiogram (ECG) signals [1].

In this study, we focused on PLI in large sEMG arrays. The PLI 60 (50) Hz fundamental and its harmonics clearly corrupt the usable frequency bandwidth of sEMG signals in the range of 20 Hz to 450 Hz. Based on one sEMG sensor, common methods to reduce PLI consist to use frequency notch filters or to employ a reference sEMG as in [1]. For this kind of multivariate sEMG systems, the literature is very limited and the frequency notch filter is the prevalent simple solution. However, it is generally preferable to minimize the amount of filtering [5]. Contrary to the single channel case there is little research reported on the topic of removal of PLI in this context of large multichannel systems.

The PLI generally comes from a low number of well-correlated sources. In linear algebra terms, the PLI multivariate signal has a low dimensionality. In beamforming terms, it has a low spatial dimension. Also, the PLI has very narrow frequency bands for fundamental frequency and its harmonics. These characteristics of the PLI lead to think that the combination of spatial (beamforming) [2] and frequency filtering could be used to isolate it from the desired signal.

Beamforming principles have been explored in [3]-[6] for EEG systems. The beamforming method of principal component analysis (PCA) was used. PCA decomposes the signals by minimizing the correlation and order them by variance (i.e. power). In the case of EEG, the most powerful signals obtained after decomposition should contain the PLI. Independent component analysis (ICA) was necessary to further isolate the PLI among the results of the PCA. No similar approach has been done for sEMG systems. In the case of EEG, the PLI is generally much stronger than the desired signals. It is hence easier to isolate the PLI as being one of the strongest components. In the case of sEMG, the interference is generally of the same order of magnitude as the desired signal. The use PCA without prior filtering would lead to an ordering problem as in ICA.

A similar approach was used for ECG [7]-[11]. There, the signal power is stronger, but the number of sensors is very limited. Also, the ECG signal comes from a relatively localized source. It is therefore easier to use ICA to separate the ECG and PLI which are two well-defined sources. Even then, the ordering problem of ICA is still complex [9]. For sEMG signals, the desired signals come from a high number of sources (motor units) distributed over a larger region. This is particularly true for the low back region. The different motor units are more or less synchronized, but clearly less than the different components of the ECG. The ICA cannot easily be used with sEMG arrays.

For these reasons, we propose to apply a PCA based beamforming only in the frequency band of the PLI, without use of ICA. This approach is very straightforward, with few parameters and present many advantages:

- the method is not sensible to the choice of the parameters.
- the subspace selection is much easier than ICA based method since the PLI should be found by simple variance calculation. There is no major ordering problem.
- an error of subspace selection is of low impact since if the PLI is not the strongest signal in the PLI frequency band, than its impact is minor.

- In the large sensor array context, losing a few spatial dimensions of the desired signal in a narrow band has a negligible impact. Choosing the wrong subspace in ICA can lead to major error.

An analysis of the performances of the proposed method is done by adding a synthetic interference signal over real-world experimental data from our depicted experimentation on LBP patients at frequencies where the interference is generally not present. The performances are compared to a standard notch filter. The method of spatio-frequency filtering presented was designed for sEMG large sensor array applied on the low back region. The use of ICA was unnecessary to isolate the PLI. The approach should be readily adapted for EEG and ECG systems. The ICA could be incorporated to the method for those systems.

The paper is organized as follows; the proposed system is presented in Section 2. The analysis of the proposed filter is postponed to Section 3, while Section 4 draws some brief conclusions.

2. SPATIO-FREQUENCY NOTCH FILTER

The spatio-frequency notch filter proposed in Fig. 1 is used to cancel the signal in a limited frequency band in only one or few spatial directions. A spatial dimension is equivalent to a linear combination of measurement channels [2]. As an example, for 56 differential measurements matrix used, there are 56 spatial dimensions.

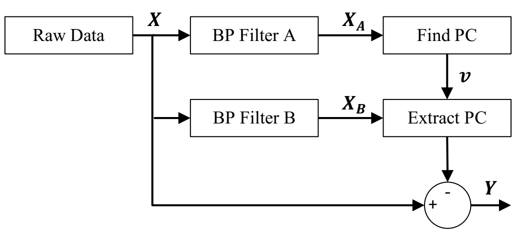

Fig. 1. Structures for the proposed spatio-frequency notch filter

In order to find the best spatial direction to be removed, the data is first passed through a narrow band-pass (BP) filter at the central frequency of the interference, the BP Filter A in Fig. 1. This ensures that the major part of the filtered signal is composed of interference, i.e. it minimizes the signal to interference ratio (SIR). After, on the filtered data, a search of the spatial direction (PC – principal component) where the signal is the strongest is done. PCA method is a common way of finding it. This direction is likely to contain most of the interference, especially if there is only one spatial source of interference. Then the raw data are filtered again with another band-pass filter of wider band, the BP Filter B. The part of the wideband filtered signal which is in the spatial direction found by PC extraction is subtracted from the raw data.

The algorithm can be applied for each undesired interference frequencies, such as harmonic frequencies. It can also be applied more than once at the same frequency when the interference has higher order of spatial dimensions.

A) Band-Pass Filtering

The Fast Fourier Transform (FFT) is used for the bandpass filters. The undesired frequencies are set to zero in the frequency domain. The filtered signal is then returned in the time domain by applying the Inverse FFT (IFFT). This is reasonable for an offline data analysis. Also, since the time span of the data was large, windowing was unnecessary.

B) Principal Component

The PCA method first requires the estimation of the covariance matrix. It is the spatial correlation which is considered. The general equation for the covariance matrix for the system of Fig. 1 is:

$$\boldsymbol{\Sigma} = E[(\boldsymbol{x_A} - E(\boldsymbol{x_A}))(\boldsymbol{x_A} - E(\boldsymbol{x_A}))^T] \tag{1}$$

where E[•] denotes the statistical expectation operator and $\boldsymbol{x_A}$ is a $M \times 1$ vector related to the output of the BP Filter A with M the number of channels. However, because the signal was previously passed through an ideal band-pass filter, it has no mean. For the system of Fig. 1, under the assumption of stationarity, the estimator of $\boldsymbol{\Sigma}$ is:

$$\boldsymbol{Q} = \frac{1}{N}\boldsymbol{X_A}\boldsymbol{X_A^T} \tag{2}$$

where $\boldsymbol{X_A}$ is a $M \times N$ matrix related to the output of the BP Filter A, with N for the number of data per channel and M the number of channels. The unbiased version of the estimated covariance matrix is used due that mean is null. An eigendecomposition of the estimated covariance matrix is:

$$\boldsymbol{Q} = \boldsymbol{VDV^{-1}} \tag{3}$$

The columns of the matrix $\boldsymbol{V}$ are formed by the eigenvectors of $\boldsymbol{Q}$, ordered by the power of the eigenvalues found in $\boldsymbol{D}$. The first column vector of $\boldsymbol{V}$ is written $\boldsymbol{v}$ and is the desired direction. The vector $\boldsymbol{v}$ is unitary.

C) Removal of the Spatio-Frequency Dimension

To remove the spatio-frequency dimension associated to the interference, the second band-pass filter, BP Filter B, is projected on the direction of the principal component $\boldsymbol{v}$, and The data with interference removed $\boldsymbol{Y}$ is also an $M \times N$ matrix

$$\boldsymbol{Y} = \boldsymbol{X} - \boldsymbol{v}(\boldsymbol{v^T X_B}) \tag{4}$$

Here $\boldsymbol{X}$ is the $M \times N$ matrix of the original raw data and $\boldsymbol{X_B}$ is the matrix of the data filtered by the BP Filter B.

It could be possible to remove simultaneously many spatial dimensions. However, doing it in different steps allows changing the bandwidth of the filters for each spatial dimension. Let's note that the removal of principal components by reconstruction using remaining components, as usually done in PCA based denoising, would be more complex and less precise because most PC are kept.

3. EXPERIMENTAL RESULTS

In our case, we take advantage of a high number of sEMG sensors or high-density sEMG to remove PLI. Indeed, in our laboratory we applied an 8×8 sEMG array (Model ELSCH06NM3, 10 mm inter-electrode distance (IED), OT Bioelettronica, Italy), which gives 56 differential channels, on lumbar erector spinae muscles of a low back pain (LBP) patient [12]-[14] in order to study its neuromuscular strategy during an endurance task. In order to analyze the performances of the algorithm in a realistic context, two scenarios are studied. In the Scenario 1, we applied the proposed method to real data from a typical large sEMG array signal to remove the data interferences. In the Scenario 2, a new simulated interference, known, has been added and the spatio-frequency notch filter is applied to remove the simulated interference in order to evaluate the performances.

A) Scenario 1: Real-World Noisy sEMG Grid Channels

The known interference is added in frequency regions where no interference was present in the original measured data. The proposed spatio-frequency notch filter is compared to the conventional frequency notch filter. There are 56 differential channels sampled at 2048 Hz. The Fig. 2 shows, as an example, the data from two EMG differential channels, in the time domain. The 56 channels are similar. Fig. 3(a) shows the frequency domain representation of the data (in absolute value). For clarity, the frequency axis is displayed up to 600 Hz instead of the 1024 Hz allowed by the sampling frequency. Interference spikes can be seen principally at 120 Hz and 300 Hz. Furthermore, other harmonics of 60 Hz are present. However, no dominant interference is found in the 60 Hz itself, a common situation when PLI is mostly produced by lighting equipment. Although the spikes are very narrow (either in the -3 dB or in 99% power bandwidth sense), its impact on the signal has a significant bandwidth. Fig. 4 compares on experimental data in Fig. 4(a), the results of the spatio-frequency notch filter in Fig. 4(b) and by standard notch filter in Fig. 4(c). The standard notch filter completely loses the desired signal in the interference bandwidth. Moreover, it can be seen that the interference at 300 Hz has more power than the desired signal over about 6 Hz of bandwidth. The full bandwidth of the significant interference should be even larger.

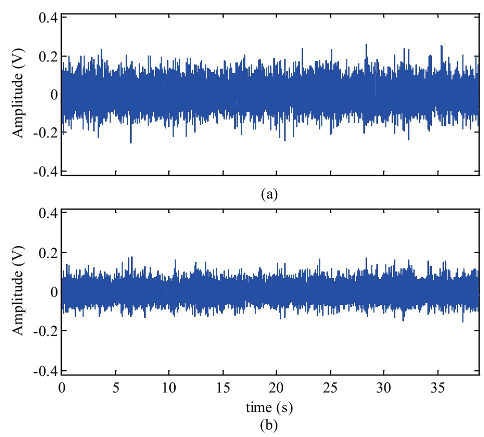

Fig. 2. Raw data in the time domain of two measurements of differential channels sampled at 2048 Hz.

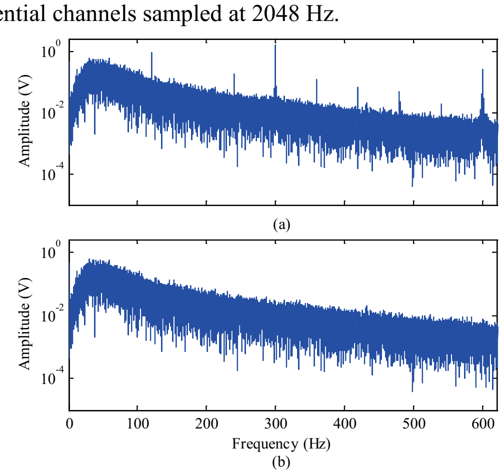

Fig. 3. Raw data (a) and data with interference removed by the proposed spatio-frequency notch of one measurement channel in the frequency domain (b).

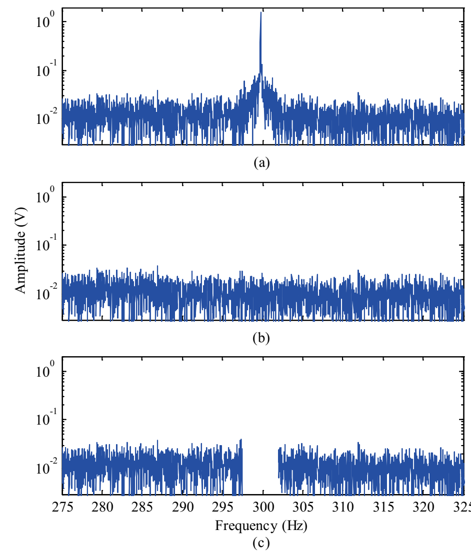

Fig. 4. Zoomed version around 300 Hz of Fig. 3a (a) and data with interference removed by the proposed spatio-frequency notch Fig.3b (b) and by standard notch (c) of one measurement channel.

B) Scenario 2: Synthetic noisy sEMG grids

To evaluate the interference removing with the proposed and reference methods, an interference signal has been synthetically added to approximate typical real world interferences. The sine wave used had variable amplitude and phase. If PLI was a pure sinus signal, it would be very easy to remove it. The variations levels were chosen to make the simulated power spectrum similar to the experimental one (except for the central frequency).

The simulated interference frequency representation is shown in Fig. 5(a) for 110 Hz centered interference. Fig. 5(b) shows the sum of the data and simulated interference. The interference is produced in all of the 56 measurements with random scaling for amplitudes (Gaussian) and random phases (uniform). For the performance analysis, the mean square error (MSE) is considered. The MSE is normalized by the power of the interference. Hence, a normalized MSE of 0 dB means that the power of the error is equal to the power of the interference. Let's note that a positive MSE in dB can be interpreted as the desired signal that has been canceled more than the interference and is an undesired result.

In Fig. 6, the performances of the proposed spatio-frequency notch filter are compared to the performances of the conventional and usually used frequency notch filter. The bandwidth of the standard frequency notch filter is varied as

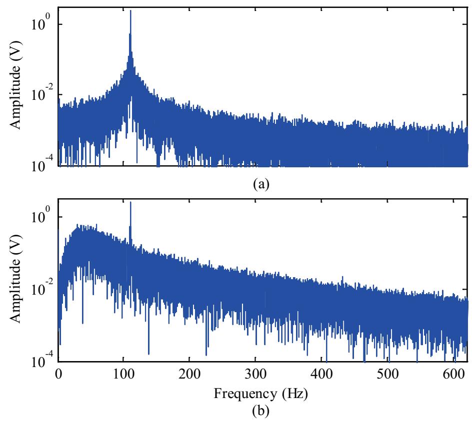

Fig. 5. Simulated interference (a) and data plus simulated interference (b) of one measurement channel. The interference has been created synthetically while the sEMG signals are experimental.

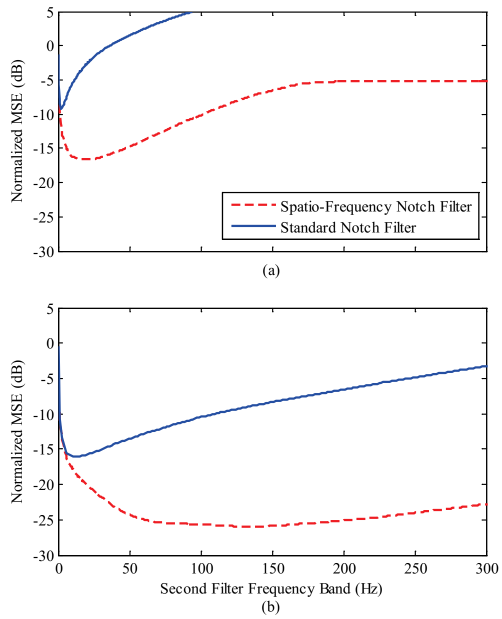

Fig. 6. Comparison between the proposed spatio-frequency notch filter (dashed line) and the standard notch filter (solid line) for interference suppression at 110 Hz (a) and 330 Hz (b).

the bandwidth of the BP Filter B of the spatio-frequency notch filter with 0.5 Hz for BP Filter A bandwidth. Two interference frequencies are considered, 110 and 330 Hz, the central frequencies are 110 Hz in Fig. 6(a) and 330 Hz in Fig. 6(b). In both cases, the spatio-frequency notch filter gives superior results than the standard frequency notch filter. At 110 Hz, the difference of MSE at the respective optimal frequency band is about 8 dB at 110 Hz and about 10 dB at 330 Hz. It can also be seen that the interferences are more easily removed at high frequency because the main power of the signal is at low frequency. Moreover, at low frequency, the performances are much more sensitive to the bandwidth. For instance, for the interference at 330 Hz, there is not a significant difference between the MSE found for a second filter frequency band between 50 Hz and 250 Hz.

Finally, the impact of the first filter frequency band (BP Filter A) is discussed. It is observed that for both 110 Hz and 330 Hz interference, the best frequency band is the narrowest. However, a too narrow band needs a better knowledge of the center frequency of the interference.

4. CONCLUSION

In this paper, we have outlined an approach to isolate the PLI in a sensor array by exploiting the correlation of the interference between the channels and its narrow band frequency characteristic. This allows keeping most of the desired signal, even at the frequency of the PLI. The proposed technique has been shown to be effective on real data. Also, the performances were studied with simulated interference added to real data. We expect that the basic principles can be extended to EEG and ECG systems and to more general contexts, such as for dynamic task, where the subject (hence the sensors) is in movement. In this case, the beamforming and the filtering should be adaptive.

Acknowledgment – The authors wish to thank the Natural Sciences and Engineering Research Council of Canada and *Fonds Excellence* UQTR for their financial support.

REFERENCES

[1] C. Kezi Selva Vijila, P. Kanagasabapathy, E. Selva Kumar, “A Survey of Interference Cancellation in Biosignals,” Int. Journal of Reviews in Computing, vol.7, pp. 64-83, Sept. 2011.

[2] B. D. Van Veen and K. M. Buckley, "Beamforming: a versatile approach to spatial filtering," in IEEE ASSP Magazine, vol. 5, no. 2, pp. 4-24, April 1988.

[3] M.B.I. Reaz, M.S. Hussain, and F. Mohd-Yasin, “Techniques of EMG Signal Analysis: Detection, Processing, Classification and Applications,” Biological Procedures Online, pp. 11-35, 2006.

[4] S. Hu, M. Stead and G. A. Worrell, "Automatic Identification and Removal of Scalp Reference Signal for Intracranial EEGs Based on Independent Component Analysis," IEEE Trans. on Biomedical Engineering, vol.54, pp. 1560-1572, Sept. 2007.

[5] S. Hu, M. Stead, G.A. Worrell, “Removal of Scalp Reference Signal and Line Noise for Intracranial EEGs,” IEEE Int. Conf. on Networking, Sensing and Control, pp.1486-1491, April 2008.

[6] C. Guerrero-Mosquera, A. Navia Vazquez, “Automatic removal of ocular artifacts from EEG data using adaptive filtering and independent component analysis”, European Signal Processing Conference, pp. 2317-2321, Aug 2009.

[7] A. S. Barhatte, R. Ghongade and S. V. Tekale, "Noise analysis of ECG signal using fast ICA," Conf. on Advances in Signal Processing, Pune, 2016, pp. 118-122.

[8] W. Sanxiu and J. Shengtao, "Removal of Power Line Interference of ECG Signal Based on Independent Component Analysis," Int. Workshop on Education Technology and Computer Science, Wuhan, Hubei, 2009, pp. 328-330.

[9] T. He, Clifford and L. Tarassenko “Application of ICA in Removing Artefacts from the ECG”, Neural computing and Application, vol. 15 issue 2, April 2006

[10] A. K. Barros, A. Mansour, and N. Ohnishi, “Removing artifacts from Electrocardiogramic signals using independent components analysis,” Neurocomputing, vol. 22, 1998.

[11] M.P.S. Chawla “PCA & ICA Processing Methods For Removal Of Artifacts and Noise in ECG”,Applied Soft Computing Journal Vol.11,2011

[12] F. Nougarou, D. Massicotte, M. Descarreaux, “Detection Method of Flexion-Relaxation Phenomenon Based on Wavelets for Patients with Low Back Pain,” EURASIP J. on Advances in Signal Processing, pp. 1-17, July 2012.

[13] M. Caza-Szoka, D. Massicotte and F. Nougarou, "Naive Bayesian learning for small training samples: Application on chronic Low Back Pain diagnostic with sEMG sensors," 2015 IEEE Int. Instrumentation and Measurement Technology Conference (I2MTC) Proceedings, Pisa, 2015, pp. 470-475.

[14] M. Caza-Szoka et al., "Surrogate analysis of fractal dimensions from SEMG sensor array as a predictor of chronic low back pain," Int. Conf. of the IEEE Engineering in Medicine and Biology Society (EMBC), Orlando, FL, 2016, pp. 6409-6412.